

ARTICLE INFO:

Received : July 26, 2018

Revised : August 22, 2018

Accepted : March 13, 2019

CT&F - Ciencia, Tecnología y Futuro Vol 9, Num 2 December 2019. pages 79 - 88

DOI : <https://doi.org/10.29047/01225383.181>



ctyf@ecopetrol.com.co

PERFORMANCE ANALYSIS OF A COMMERCIAL FIXED BED DOWNDRAFT GASIFIER USING PALM KERNEL SHELLS

ANÁLISIS DE DESEMPEÑO DE UN GASIFICADOR COMERCIAL DE LECHO FIJO EN EQUICORRIENTE UTILIZANDO CUESCO DE PALMA

Verdeza-Villalobos, Arnaldo ^{a, b*}; Lenis-Rodas, Yuhan-Arley ^{b, c}; Bula-Silvera, Antonio-José ^b; Mendoza-Fandiño, Jorge-Mario ^d; Gómez-Vásquez, Rafael-David ^e

ABSTRACT

This work analyzes the use of palm kernel shells (PKS) produced by the Colombian palm oil mill industry, for purposes of fueling a commercial downdraft fixed bed gasifier (Ankur Scientific WGB-20) designed to operate with wood chips. Operational parameters such as hopper shaking time, ash removal time, and airflow were varied in order to get the highest gasifier performance, computed as the ratio between producer gas chemical energy over biomass feeding energy. Experiments were carried out following a half fraction experimental design 2^{4-1} . Since these parameters affect the equivalence ratio (ER), behavior indicators were analyzed as a function of ER. It was found that the shaking time and airflow had a significant effect on higher-heating-value (HHV) and process efficiency, while the removal time is not significant. Highest performance for palm shell was reached at ER=0.35, where the resulting gas HHV and process efficiency were 5.04 MJ/Nm³ and 58%, respectively.

RESUMEN

En este trabajo se analiza el uso de cuesco de palma africana (proveniente de la industria colombiana del aceite de palma), como combustible para un gasificador comercial downdraft (Ankur Scientific WGB-20). Se plantea un diseño experimental fraccionado 2^{4-1} , variando el flujo de aire, el tiempo de vibración de la tolva y remoción de cenizas, con miras a obtener el mayor rendimiento, estimado mediante la relación entre el contenido energético del gas y la biomasa utilizada. Dado que los factores manipulados afectan la relación de equivalencia (ER), los principales indicadores se analizan como función de este. De acuerdo con los resultados, sólo el tiempo de vibración y el flujo de aire tienen un efecto significativo sobre el rendimiento y poder calorífico superior (PCS) del gas de síntesis. El rendimiento más alto se encontró para ER=0.35, donde el PCS del gas y la eficiencia del proceso fueron de 5.04 MJ/Nm³ y 58%, respectivamente.

KEYWORDS / PALABRAS CLAVE

Fixed bed downdraft gasification |
Kernel shells | African palm
Gasificación en lecho fijo equicorriente |
Cuesco | Palma africana

AFFILIATION

^aDepartamento de Ingeniería Industrial, Universidad Simón Bolívar, Carrera 59 No. 59-65, Barranquilla, Colombia.

^bDepartamento de Ingeniería Mecánica, Fundación Universidad del Norte, Km.5 Vía Puerto Colombia, Barranquilla, Colombia.

^cFacultad de ingeniería, Institución Universitaria Pascual Bravo, Calle 73 No. 73A - 226, Medellín, Colombia.

^dDepartamento de Ingeniería Mecánica, Universidad de Córdoba, Carrera 6 No. 77- 305 C.P 230002, Montería, Colombia.

^eDepartamento de Ingeniería Mecánica, Universidad Pontificia Bolivariana (Montería), Carrera 6 No. 97 A - 99, Montería, Colombia.

*email: averdeza@unisimonbolivar.edu.co

1 INTRODUCTION

Environmental issues related to fossil fuels as well as the potential fuel shortage scenario encourage research into alternative fuels and improvements in conversion technologies. Among the alternatives for gas fuel generation from biomass, gasification is one of the most proven and efficient processes. Air gasification (i.e. a process where air is used as the gasifying medium) yields a gas with a low HHV (~5.0 MJ/Nm³) suitable for feeding conventional combustion engines after minor modifications. Additionally, this process can use industrial and agroforestry waste as feedstock, increasing its environmental benefits. Since Colombia is the fourth largest palm oil producer in the world, waste from this industry has very high potential as an energy source. This industry processes about 5423 million tons of fresh fruit bunches per year [1], with oil being the main product extracted (about 21 wt. %), and the remaining 79% considered waste. Around to 1188 million tons of waste are produced every year. This is comprised by 721000 tons of fibers and 352000 tons of palm kernel shells (PKS) [2]. The latter has a real density of between 1500 to 1530 kg/m³ and is composed of a high content of volatile material, fixed carbon and oxygen, as well as low ash and some moisture. These characteristics, added to the waste's high availability, are the main indicators regarding its high potential for the production of sustainable energy [3],[4].

Using very heterogeneous granular fuels for gasification processes could lead to certain issues; some of the most common are high tar generation, low gas HHV and operational instabilities that could even lead to flame extinction [5]. These issues can be addressed through fuel pretreatments such as drying, size homogenization and densifying. Nevertheless, all of them imply using additional equipment that affects the economic viability of projects [6]. Due to its low tar production and resulting gas quality, fixed bed downdraft gasifiers are the most suitable alternative to generate power from biomass in low power levels (<2 MWe) [7],[8]. Simplicity in both design and construction are also among its main advantages, reducing initial investment and therefore power generation costs [9]. On the other hand, process instabilities are the major drawback. They usually arise when very heterogeneous biomasses are used, encouraging bridging and channeling formation in the feeding hopper, which results in localized high temperature zones. These undesirable phenomena result in fuel blockage and lead to flame extinction [10], [11].

Industrial waste has been previously proposed as fuel for downdraft fixed bed reactors. Generally, process response is analyzed as a function of equivalence ratio, particle size distribution and gasifying agent. Lenis et al. [12] gasified sawdust-woodchips mixtures under several air flow rates. They encountered sawdust fluidization when sawdust concentration was higher than 30%. Ouadi et al. [13] evaluated power and heat generation from paper industry waste mixed with woodchips, and producer gas HHV around 7.3 MJ/Nm³ at 80% residues and 20% woodchip mixture were reported. However, fuel agglomeration and blockage was found

during some experiments. These issues were related to polymeric particle presence in some of the tested blends. Feeding a 50.0 KW_{th} gasifier with coconut – rubber seed shell mixtures, Jeya et al [14] analyzed process performance through theoretical and experimental approaches. Authors found performance for residuals that was comparable with that reported for wood biomass at equivalence ratios from 0.2 to 0.3. Sreejith et al. [15] carried out a theoretical study using coconut shells and fibers, bamboo and eucalyptus with air and air-steam mixtures as gasifying agents. Among the biomasses analyzed, the highest energy and exergy efficiencies were from coconut shells. A decrease in overall process efficiency was noticed when steam was added to the reactor, and this was related to low process temperature.

According to literature, a lot of industrial waste cannot be used individually as fuel for gasifiers, as it necessary to carry out pretreatments or use mixtures containing materials with better properties. However, similar performance to those related to lignocellulosic biomass may be achieved using some pure raw waste such as palm kernel shells due to its physicochemical properties [16]. High temperatures and biomass densities as well as homogenous particle size were related to high process performance. On the other hand, it has been found that process performance is close to the optimal when ER is around 0.3 [17]–[19].

Since the air-to-biomass ratio is one of the variables that has a stronger effect on gasifier performance [14], [20], in commercial downdraft gasifiers, the biomass feeding rate and airflow can be changed independently, which means that the user is able to set the thermochemical state of the process, seeking the maximum performance. However, biomass feeding rate is limited by biomass consumption rate [21] which in turn depends on air flow, and thus both variables must be manipulated carefully. Although gasifier has a vibrating system to facilitate biomass flow, once biomass was fully settled, the consumption rate does not change as a function of the shaking time. When this condition is reached, the user cannot control the rate to feed the fuel, and the hopper vibration only induces noise to the process. As with the shaking system, the time for ash removal can be changed (on-off settings) to achieve the best process performance. Nevertheless, there is no certainty regarding the best configuration when a biomass other than the one suggested by the gasifier manufacturer is used. Moreover, most studies carried out had been focused on process variables, mainly ER, temperature, pressure and residence time. In this work, changes in the operational parameters of a commercial gasifier fueled with palm shell biomass were analyzed. This work was conducted using a 2⁴⁻¹ experimental design with three central points. After significant factors were established, the equivalence ratio, biomass feeding rate and reaction temperature effects on process efficiency and producer gas quality were analyzed. This kind of study makes it possible to identify optimum operational conditions when the biomass differs from the manufacturer recommendation.

fuel for the process. This system is provided by Ankur Scientific to generate power from woodchips. Three K-type thermocouples and a hot wire sensor were installed to measure temperatures and airflow respectively, in order to analyze the system behavior. In a Downward gasifier, the produced gas goes through a filtering system where

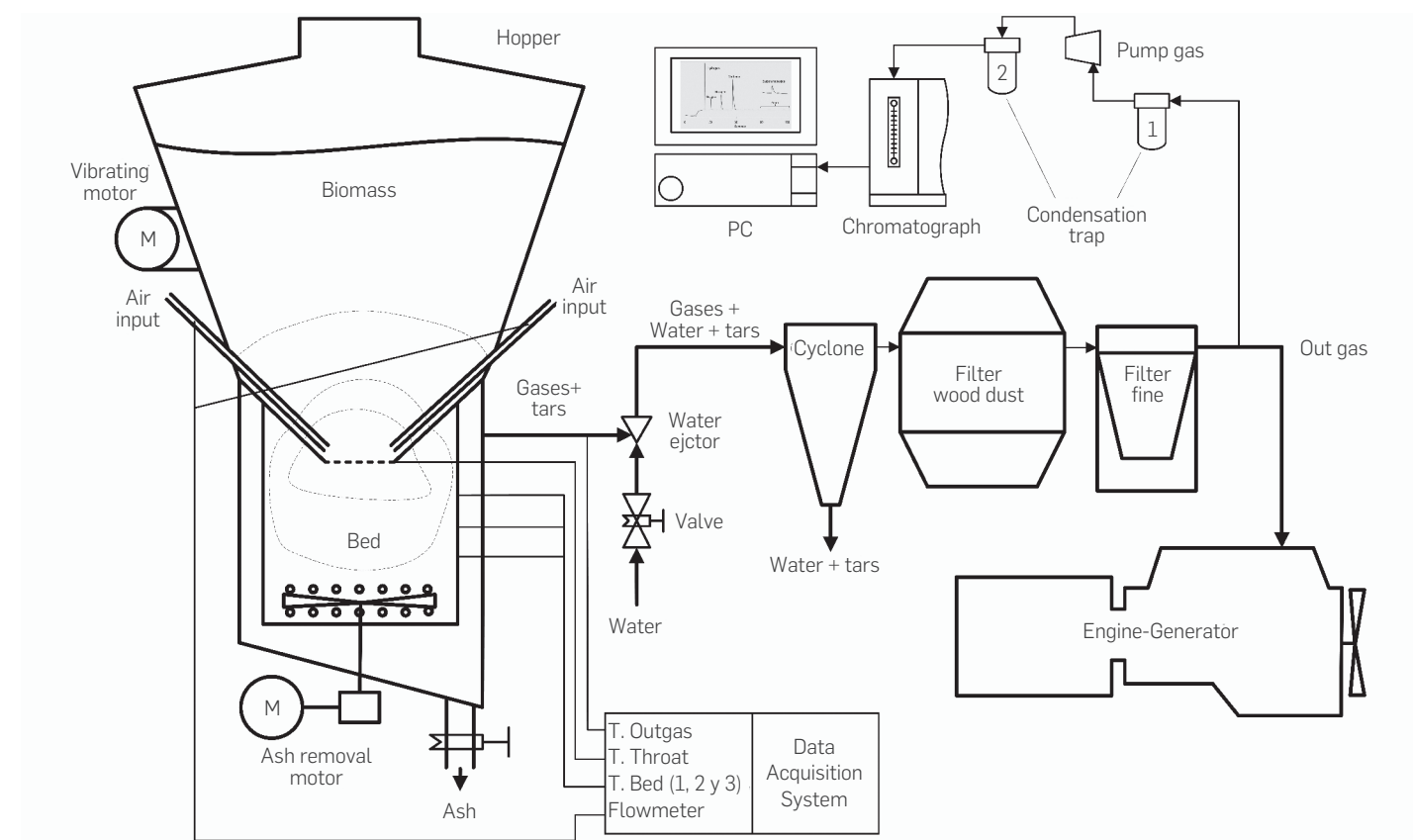


Figure 1. Experimental facility diagram.

particles and tars are removed. Then, an Agilent 490 Micro-GC measures gas composition (see Figure 1). The gasifier consists of the following components: a 420 liters storage hopper, a two-wall cylindrical reactor, a water ejector system, a cyclone and a couple of filters, all of them connected through steel tube pipe.

The storage hopper has a vibrating system that keeps solids flowing downwards, and two air inputs at the bottom for feeding air to the combustion zone. The hopper has a throat at its bottom, and under the throat there is a two-wall cylindrical reactor where reduction reactions take place. Next to the combustion zone there is a grate; gas and ashes cross this grate when leaving the reactor. To allow air and gas to flow through the gasifier bed, a water ejector system is used. This enables reduction of the pressure at the gas exit, inducing gas flow through reactor. In addition to its gas drag function, water also helps remove fine ash and tar impurities from the gas. Shaking and ash removal systems have electrical motors with programmable on-off switches. The shaking motor makes it possible to set the switch-off time only while the on-time was defined at 60 seconds by the manufacturer. Meanwhile, the ash removal motor allows you to set both on and off switching times.

STATISTICAL EXPERIMENTAL DESIGN AND TEST PROCEDURE

The main aim of this work was to determine the effect of the operational variables, shaking time, ash removal and airflow on

gas HHV, efficiency and biomass consumption rate. A factorial experimental design 2⁴⁻¹ (fourth factors, three levels and three central points) was developed for this purpose.

First, the study was focused on establishing the significance level for each experimental factor, ensuring three degrees of freedom for random error. Given the operational limitations of the equipment, a set of factors and their levels were chosen as shown in Table 1.

100 kg of PKS were loaded into the gasifier hopper before each experimental run. Then, all the experimental factors were set up and the data acquisition system was initiated. The airflow system was switched on and then, a flaming torch was placed at the air inputs, leading to initiation of the biomass gasification process.

The test duration was 180 min. However, only data after 60 min from start was analyzed to guarantee normal operation conditions (steady state for gas concentrations and HHV). The remaining ash, charcoal and biomass were weighted after each run, aiming to establish the biomass consumption rate (\dot{m}_{bms}), computed as the difference between initially fed mass (100 kg) and the remaining biomass divided by the test duration, 180 min. Similar methodology was used in [22]. It is worth noting that even charcoal was not consumed; its weight was checked after every test.

HHV_{gas} for each test was computed as the arithmetic average of the heating values measured during quasi-stable conditions. This parameter was estimated indirectly using the gas concentration (x) and the heating value of each fuel species present in the

gas (see Equation 1). These samples were analyzed through gas chromatography every 3 minutes.

$$HHV_{gas} = \sum_i x_i HHV_i, \therefore i = H_2, CO, CH_4, C_2H_6, C_3H_8 \quad (1)$$

Process efficiency (η_I) was computed as the rate between the output gas energy reactor and the input biomass energy supplied (see Equation 2). Efficiency does not consider the gas sensible energy, because gas usually needs to be cooled with water before being used in internal combustion engines. Gas flow was computed in accordance with the methodology presented in [19].

$$\eta_I = \frac{E_{out}}{E_{in}} = \frac{\dot{m}_{gas} \cdot HHV_{gas}}{\dot{m}_{bms} \cdot HHV_{bms}} \quad (2)$$

Equivalence ratio (ER) was computed as per Equation 3.

$$ER = \frac{(\dot{m}_{air}/\dot{m}_{bms})_{real}}{(\dot{m}_{air}/\dot{m}_{bms})_{stq}} \quad (3)$$

BIOMASS

Biomass chemical properties were obtained in line with ASMT standard procedures (See Table 2). The proximate analysis was carried out in accordance with standard ASTM D 7282-15 and determination of the HHV in kJ/kg was carried out as per ASTM D 7282-13. Ultimate analysis was carried out in an elemental analyzer, Exeter Analytical CE 440, adapted to the ASTM D 5373 standard, sulfur content with ASTM D 4239-14 Method A and oxygen content was obtained by difference.

Table 1. Experimental conditions

Controlled factors		
Experimental factor.	Factor level	
	low (-1)	high (+1)
Shutdown time for hopper vibrating motor, t_{voff} (s).	1200	3600
Operation time for ash removal motor, t_{ron} (s).	12	42
Shutdown time for ash removal motor, t_{roff} (s).	40	200
Airflow, F_{air} (Nm ³ /h).	10.99	21.07
No-controlled factors		
Operation time for hopper vibrating motor.	60 s	
Bed pressure- atmospheric pressure.	101.32 kPa.	
Angular velocity and mass load coupled to vibrating motor.	1370 rpm – 1.47 N	
Angular velocity and torque for ash removal motor	1.00 rpm – 3.92 N·m	
Biomass moisture content.	6-8 wt.%	
Biomass physical and chemical properties.	Elemental analyses, HHV, granulometric, density, porosity and packing factor (see tables 1 and 2).	
Environmental temperature	30°C – 36°C	
Air relative humidity	75% - 85%	

Table 2. Chemical properties of Palm Shell.

Proximate analysis			Ultimate analysis		
Parameter	Value (wt. %)	Standard	Component	Value (wt. %)	Standard
Moisture	5.91		Carbon	48.75	ASTM D 5373
Volatile	76.82	ASTM D 7282-15	Hydrogen	5.55	
Fixed carbon	13.71		Nitrogen	0.80	
Ash	3.56		Sulfur	0.10	ASTM D 4239-14 Method A
HHV (kJ/kg)	19690	ASTM D 7282-13	Oxygen	35.33	by different

The physical properties of the biomass were measured experimentally, and they are presented in Table 3. Apparent and bulk densities were computed according to ASTM E873 – 82 (2013) standards and Lenis et al [19] suggestions, respectively. Real biomass density was chosen as 1500 kg/m³ and it is a constant for most wood cells; it can be measured with a pycnometer according to ASTM D854 – 14 (2014) or estimated using ultimate analysis and the real density of its constituent elements [23]. Biomass porosity ϵ_p and bulk porosity ϵ_b , were computed using Equations 4 and 5. Granulometric analyses were carried out using square sieves as per the INVE-123-07 standard. This methodology was used previously in [24]. These properties and the following results could be used to validate gasification models considering similar conditions presented in this work.

$$\rho_{apparent} = \rho_{real}(1 - \epsilon_p) \quad (4)$$

$$\rho_{bulk} = \rho_{apparent}(1 - \epsilon_b) \quad (5)$$

Table 3. Physical characterization of Palm shell

Properties	
Mean granulometry (mm)	4.86 ± 2.27*
Apparent density (kg/m ³)	1186
Bulk density (kg/m ³)	388
Particle porosity (ϵ_p)	0.22 **
Bulk porosity (ϵ_b)	0.67 **

* Based on media analyses for grouped data considering the particle size distribution.
** Calculate based on reference value taken from [23] and [24]

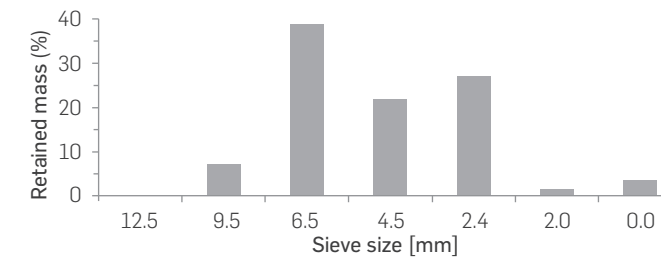


Figure 2. Particle size distribution for palm shell

3. RESULTS ANALYSIS

Tables 4 and 5 show results for palm shell gasification under the conditions presented in Table 3. Results analysis was performed following two different approaches. First, the significance levels of each factor on the equivalence ratio, HHV of the gas and process efficiency were established. Then, the equivalence ratio effects on the main process performance parameters were analyzed.

EXPERIMENTAL DESIGN ANALYSIS

The main advantage of the chosen design was the reduction of the required experimental runs. However, because of the reduction, both error degrees of freedom and the number of possible analyses were reduced. Hence, in order to verify whether a factor was significant for each of the effects, the normal probability plot method was used [25]. Table 6 shows the Analysis of Variance (ANOVA) for the significant effects identified.

Regarding the HHV of the gas, shaking off-time (t_{voff}) has a significant contribution but the airflow (F_{air}) and ash removal time variations do not exhibit a noticeable effect on the process. Similar results were found for the equivalence ratio. Airflow had the most significant effect on process efficiency (η_I).

In previous works, it has been found that HHV also depends on the airflow [14], [20]; however, in the this work it was not possible to establish this dependency. This was due to uncontrolled process variations that have higher effects on HHV rather than those caused by changes in the airflow. Also, this could be explained because the air variation was maintained close to the values recommended for gasification in a fixed bed gasifier. Figure 3 shows the Pareto charts

Table 4. Thermal performance results

Run	Experimental factors						Response variables				
	t_{voff}		t_{ron}		t_{roff}		F_{air}		Y	η_I	ER
	[s]	Level	[s]	Level	[s]	Level	[Nm ³ /h]	Level	[MJ/Nm ³]	[%]	
1	1200	-1.0	12	-1.0	40	-1.0	10.18	-1.0	4.97	40.1	0.22
2	3600	1.0	12	-1.0	40	-1.0	20.34	1.0	4.72	64.8	0.38
3	1200	-1.0	42	1.0	40	-1.0	21.37	1.0	5.54	43.3	0.21
4	3600	1.0	42	1.0	40	-1.0	11.25	-1.0	4.69	34.2	0.22
5	1200	-1.0	12	-1.0	240	1.0	21.23	1.0	5.37	54.8	0.29
6	3600	1.0	12	-1.0	240	1.0	11.25	-1.0	3.10	27.1	0.32
7	1200	-1.0	42	1.0	240	1.0	11.27	-1.0	4.84	43.0	0.27
8	3600	1.0	42	1.0	240	1.0	21.35	1.0	4.64	57.1	0.35
9	2400	0.0	27	0.0	140	0.0	16.87	0.0	5.09	57.5	0.36
10	2400	0.0	27	0.0	140	0.0	16.96	0.0	4.92	55.8	0.35
11	2400	0.0	27	0.0	140	0.0	15.68	0.0	5.04	62.8	0.36

Table 5. Produced gas properties

Run	Additional Variables											
	Process Temperature [°C]			Average gas concentration [%]							Gas flow	m_{bio}
	Throat	Bed	Gas	H ₂	O ₂	N ₂	CH ₄	CO	CO ₂	C ₂ H ₄	[kg/h]	[Nm ³ /h]
1	405.06	162.84	106.29	6.47	0.03	53.47	3.25	20.35	16.17	0.26	14.68	9.10
2	865.10	302.98	192.54	7.08	0.00	55.39	2.68	22.17	12.48	0.20	28.36	10.58
3	534.59	303.04	201.62	8.46	0.00	51.07	2.80	24.66	12.80	0.22	31.79	19.58
4	336.88	167.43	108.91	6.42	0.00	54.00	3.05	19.13	17.16	0.23	16.00	10.08
5	584.50	261.90	159.41	7.49	0.02	53.81	2.61	24.82	11.06	0.19	30.31	14.32
6	422.77	281.50	150.72	3.18	0.00	63.66	2.27	12.21	18.52	0.16	13.51	6.99
7	345.70	157.28	101.17	6.50	0.00	54.66	2.97	20.10	15.55	0.23	15.85	8.22
8	785.11	399.81	186.39	8.97	0.02	56.89	2.51	18.97	12.49	0.15	29.56	11.86
9	565.10	318.99	204.14	7.03	0.00	53.37	2.95	22.36	14.08	0.22	24.14	9.28
10	646.79	248.08	154.89	7.10	0.10	55.64	2.23	22.76	12.00	0.17	23.40	9.52
11	607.09	298.49	183.32	7.68	0.04	54.48	2.66	21.78	13.14	0.21	22.13	8.62

Table 6. ANOVA for the main process performance indicators

Variable	Source	SS	GI	MS	F ratio	P value
HHV (\bar{Y})	A: t_{voff}	1.5958	1	1.5958	7.38	0.0348
	D: F_{air}	0.8918	1	0.8918	4.12	0.0886
	Lack of fit	0.2025	2	0.1012	0.47	0.6472
	Pure error	1.2974	6	0.2162		
	Total (corr.)	3.9874	10			
Efficiency (η)	B: t_{Ron}	0.0011	1	0.0011	0.22	0.6591
	D: F_{air}	0.0714	1	0.0714	14.53	0.0089
	Lack of fit	0.0484	2	0.0242	4.92	0.0544
	Pure error	0.0295	6	0.0049		
	Total (corr.)	0.1504	10			
ER	A: t_{voff}	0.0093	1	0.0093	6.20	0.0472
	D: F_{air}	0.0057	1	0.0057	3.77	0.1001
	Lack of fit	0.0153	2	0.0076	5.07	0.0513
	Pure error	0.0090	6	0.0015		
	Total (corr.)	0.0393	10			

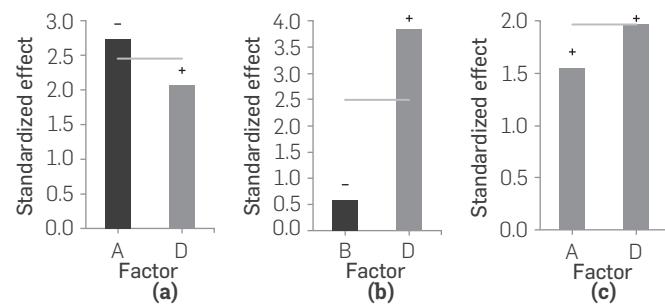


Figure 3. Standardized Pareto charts for a) HHV, b) η , and c) ER.

for standardized effects of significant factors on HHV, efficiency and ER. It is shown how the HHV decreases as t_{voff} increases. This is because under this condition, biomass entering the combustion zone is reduced moving the process toward to combustion, instead of the gasification regime. Regarding efficiency, increases in airflow (in the testing range) encourage process performance due to increases in both process temperature and rate of biomass gasification. According to literature, gasifier performance decreases significantly when operated at partial loads because energy released from the exothermal combustion reactions might not be enough to maintain proper process temperatures [26]. As expected, equivalence ratio (ER) shows a slight dependence on t_{voff} variation. This behavior is also related to process thermal conditions.

Figure 4 shows different gas concentrations and its HHV at runs 1, 3, 4 and 6. The relationship between shaking system operation and species concentration profiles is highlighted (see **Figure 4a** and **4c**). This is because when the vibration system is on, fresh biomass goes into the oxidation zone, decreasing process temperature. On other hand, a reduction was found in process variation at high airflows (see **Figure 4a** and **4b**). As the airflow increases, oxidation temperature and the flame-front thickness increases, along with a reduction in temperature variations, hence process stability increases.

Gas concentration and heating value at low both airflow conditions (low F_{air}) and biomass feeding rate (high t_{voff}) are shown in **Figure**

4d. This experimental condition resulted in high process instabilities caused by limited energy released from the oxidation sub-process, which leads to biomass bindings and temperature fluctuations (see **Figure 5**) affecting process efficiency and gas heating values. These results are due to high heat losses compared to the energy released by the biomass. According to the literature, air does not have a uniform profile when it moves through a gasifier, and the velocity profile depends on biomass size and reactor design. As a result of this reasoning, it is important to reach high bed temperatures to reduce process variations.

PERFORMANCE PARAMETERS

Equivalence ratios computed for experiments were between 0.22 and 0.38, and HHV ranged between 3.10 and 5.54 MJ/Nm³. According to previous works, for these thermochemical conditions, gas HHV values between 4.2 and 6.32 MJ/Nm³ and process efficiencies around 60% are expected [27]. **Figure 6a** shows HHV decreasing as the equivalence ratio increases; this is due to higher yield of combustion gases caused by increases in air availability. Measured HHVs were between 5.0 and 6.0 MJ/Nm³, without taking into account the atypical result measured at run 6. As mentioned previously, variations are related to equipment instabilities at these conditions that could not be avoided.

Process efficiency was aided by increases in equivalence ratio (**Figure 6b**) in the tested range. Under these conditions, the biomass-feeding rate decreases and higher process temperatures are reached. In other words, there is low energy entering the process (biomass feeding is reduced) while the process reactions are favored by the high temperatures achieved, thus releasing high power with minimum power input (**Figure 6c**).

Figure 7 shows fuel gas species concentration measured during experiments. Methane and ethane decrease as the ER increases. This is related to the increase of air entering to the process. Hydrogen and carbon monoxide do not exhibit a defined trend as a function of this parameter, which means that process instabilities have a considerable effect on the formation of these gases.

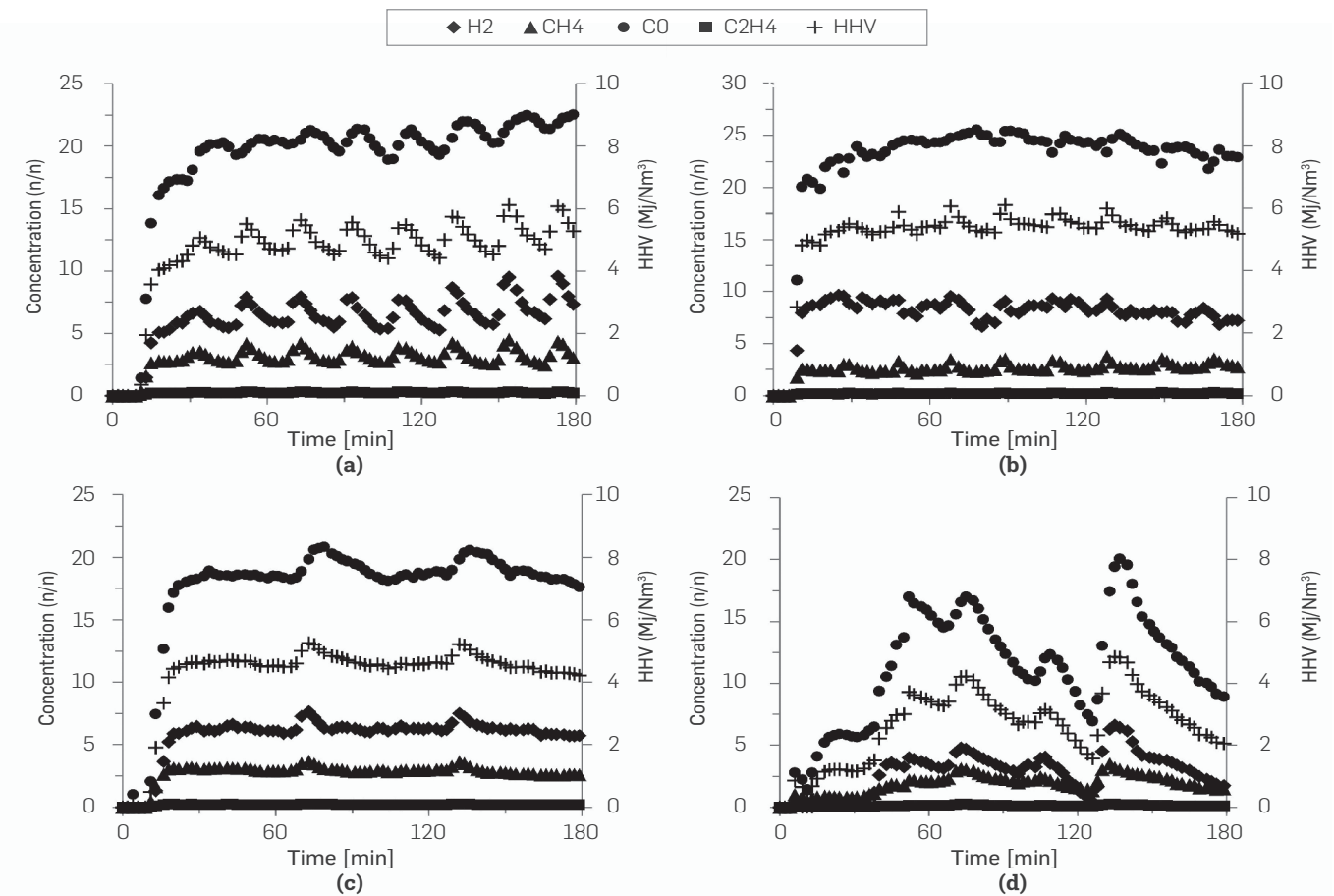


Figure 4. Concentration profile during experimental runs: a) 1, b) 3, c) 4 and d) 6.

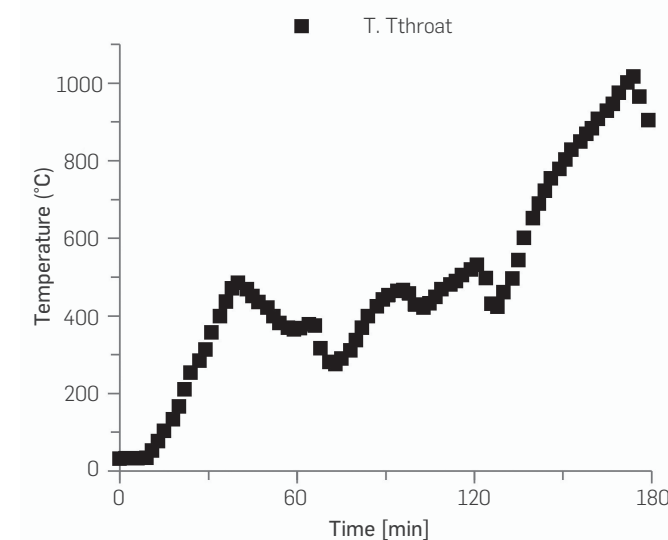


Figure 5. Pyrolysis zone temperature profile and gas HHV in run 6.

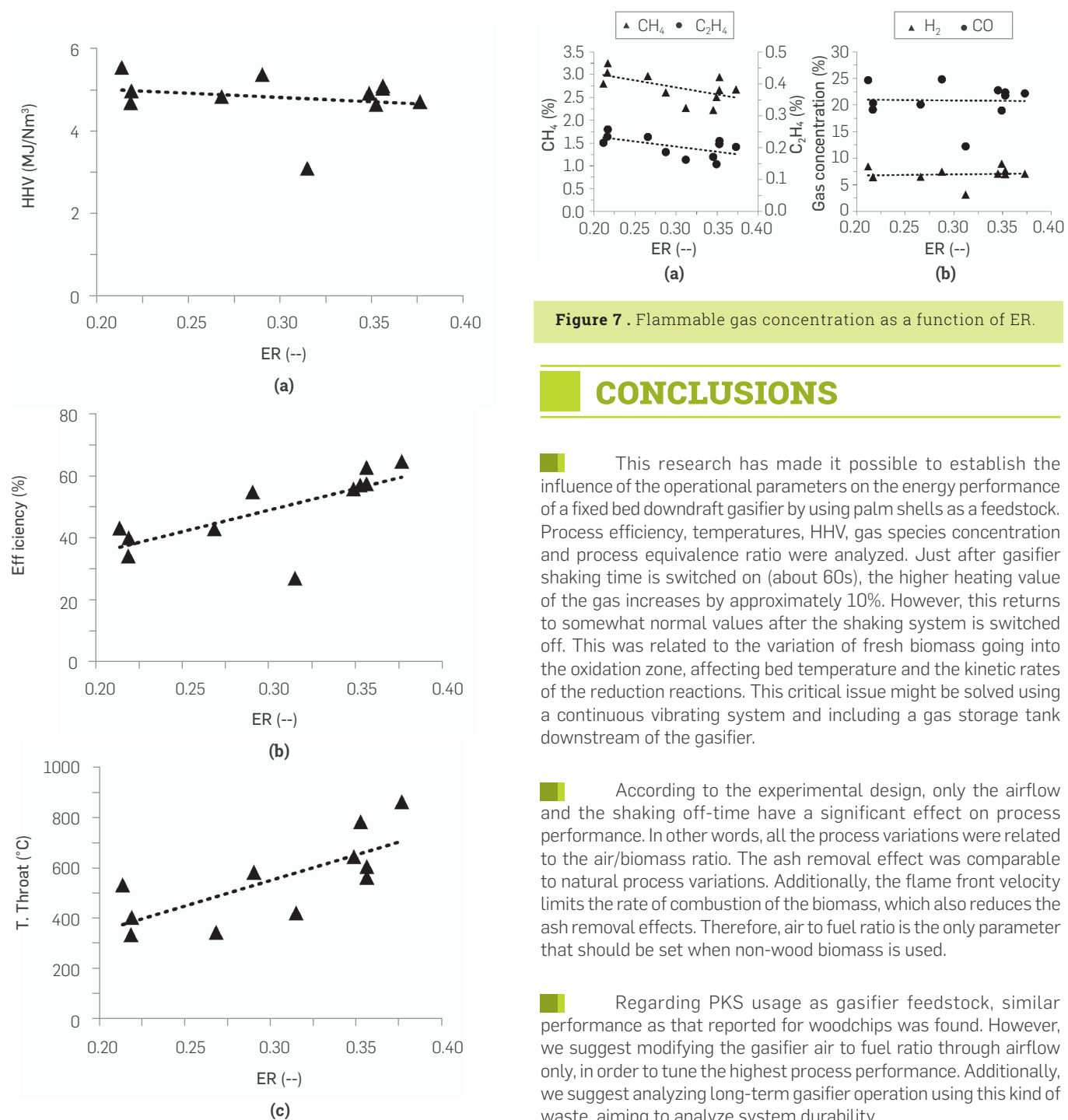


Figure 6 . Performance parameters as a function of ER.

ACKNOWLEDGEMENTS

This work was supported by Universidad del Norte, and Colciencias as a part of the research project grant 727/757 and "Fondo de Ciencia, Tecnología e Innovación - FCTel del sistema general de regalías SGR".

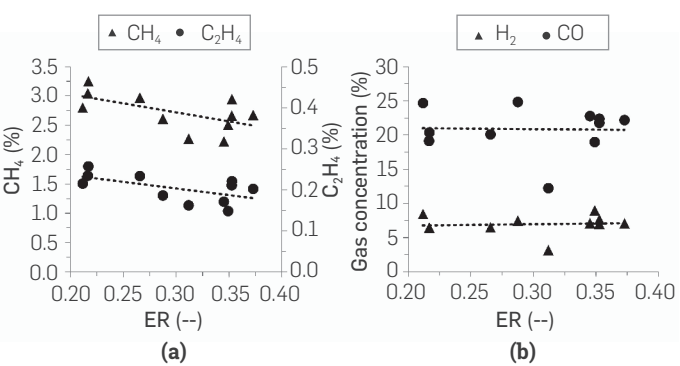


Figure 7 . Flammable gas concentration as a function of ER.

CONCLUSIONS

This research has made it possible to establish the influence of the operational parameters on the energy performance of a fixed bed downdraft gasifier by using palm shells as a feedstock. Process efficiency, temperatures, HHV, gas species concentration and process equivalence ratio were analyzed. Just after gasifier shaking time is switched on (about 60s), the higher heating value of the gas increases by approximately 10%. However, this returns to somewhat normal values after the shaking system is switched off. This was related to the variation of fresh biomass going into the oxidation zone, affecting bed temperature and the kinetic rates of the reduction reactions. This critical issue might be solved using a continuous vibrating system and including a gas storage tank downstream of the gasifier.

According to the experimental design, only the airflow and the shaking off-time have a significant effect on process performance. In other words, all the process variations were related to the air/biomass ratio. The ash removal effect was comparable to natural process variations. Additionally, the flame front velocity limits the rate of combustion of the biomass, which also reduces the ash removal effects. Therefore, air to fuel ratio is the only parameter that should be set when non-wood biomass is used.

Regarding PKS usage as gasifier feedstock, similar performance as that reported for woodchips was found. However, we suggest modifying the gasifier air to fuel ratio through airflow only, in order to tune the highest process performance. Additionally, we suggest analyzing long-term gasifier operation using this kind of waste, aiming to analyze system durability.

REFERENCES

- [1] Girón, E. A., Valderrama, M. V., Ruiz, J. D., Anuario Estadístico 2017 Principales cifras de la agroindustria de la palma de aceite en Colombia 2012-2016, Fedepalma, Colombia, Tech. Rep. ISSN 2344-8490, Oct. 2017.
- [2] Arrieta, F. R., Teixeira, F. N., Yanez, E., Lora, E. and Castillo, E., Cogeneration potential in the Colombian palm oil industry: Three case studies, *Biomass and Bioenergy*, 2007, 31 (7), 503-511. <https://doi.org/10.1016/j.biombioe.2007.01.016>
- [3] Salomón, M., Gomez, M. F. and Martin, A., Technical polygeneration potential in palm oil mills in Colombia: A case study, *Sustainable Energy Technologies and Assessments*, 2013, 3, 40-52. <https://doi.org/10.1016/j.seta.2013.05.003>
- [4] Hambali, E. and Rivai, M., The potential of palm oil waste biomass in Indonesia in 2020 and 2030, *International Conference on Biomass: Technology, Application, and Sustainable Development, IOP Conf. Series: Earth and Environmental Science*, Makassar, Indonesia, Oct. 25-26, 2017. <https://doi.org/10.1088/1755-1315/65/1/012050>
- [5] Heidenreich, S. and Foscolo, P. U., New concepts in biomass gasification, *Progress in Energy and Combustion Science*, 2015, 46, 72-95. <https://doi.org/10.1016/j.pecs.2014.06.002>
- [6] Perez, J. F., Lenis, Y., Rojas, S. and Leon, C., Decentralized power generation through biomass gasification: a technical - economic analysis and implications by reduction of CO2 emissions, *Revista Facultad de Ingeniería Universidad de Antioquia*, 2012, 62, 157-169.
- [7] Lee, U., Balu, E. and Chung, J. N., An experimental evaluation of an integrated biomass gasification and power generation system for distributed power applications, *Applied Energy*, 2013, 101, 699-708. <https://doi.org/10.1016/j.apenergy.2012.07.036>
- [8] Asadullah, M., Barriers of commercial power generation using biomass gasification gas: A review, *Renewable and Sustainable Energy Reviews*, 2014, 29, 201-215. <https://doi.org/10.1016/j.rser.2013.08.074>
- [9] Samiran, N. A., Jaafar, M. N., Ng, J. H., Lam, S. S. and Chong, C. T., Progress in biomass gasification technique - With focus on Malaysian palm biomass for syngas production, *Renewable and Sustainable Energy Reviews*, 2016, 62, 1047-1062. <https://doi.org/10.1016/j.rser.2016.04.049>
- [10] Guo, F., Dong, Y., Dong, L. and Guo, C., Effect of design and operating parameters on the gasification process of biomass in a downdraft fixed bed: An experimental study, *International Journal of Hydrogen Energy*, 2014, 39 (11), 5625-5633. <https://doi.org/10.1016/j.ijhydene.2014.01.130>
- [11] Molino, A., Chianese, S. and Musmarra, D., Biomass gasification technology: The state of the art overview, *Journal of Energy Chemistry*, 2016, 25 (1), 10-25. <https://doi.org/10.1016/j.jechem.2015.11.005>
- [12] Lenis, Y. A. and Pérez J. F., Gasification of sawdust and wood chips in a fixed bed under autothermal and stable conditions, *Energy Sources, Part A: Recovery, Utilization, and Environmental Effects*, 2014, 36 (23), 2555-2565. <https://doi.org/10.1080/15567036.2013.875081>
- [13] Quadi, M., Brammer, J. G., Kay, M. and Hornung A., Fixed bed downdraft gasification of paper industry wastes, *Applied Energy*, 2013, 103, 692-699. <https://doi.org/10.1016/j.apenergy.2012.10.038>
- [14] Jeya, V. C. and Sekhar, S. J., Performance studies on a downdraft biomass gasifier with blends of coconut shell and rubber seed shell as feedstock, *Applied Thermal Engineering*, 2016, 97, 22-27. <https://doi.org/10.1016/j.applthermaleng.2015.09.099>
- [15] Sreejith, C. C., Muraleedharan, C. and Arun, P., Energy and exergy analysis of steam gasification of biomass materials: a comparative study, *International Journal of Ambient Energy*, 2013, 34 (1), 35-52. <https://doi.org/10.1080/01430750.2012.711085>
- [16] Mohammad, N. A., Chong, C., Valera-Medina, A. and Ng, J.-H., Downdraft gasification of raw and torrefied palm kernel shell, *3rd International Conference on Power Generation Systems and Renewable Energy Technologies (PGSRET), IEEE Xplore*, Johor Bahru, Malaysia, April 4-6, 2017. <https://doi.org/10.1109/PGSRET.2017.8251798>
- [17] Pérez, J. F., Melgar, A. and Benjumea, P. N., Effect of operating and design parameters on the gasification/combustion process of waste biomass in fixed bed downdraft reactors: An experimental study, *Fuel*, 2017, 96, 487-496. <https://doi.org/10.1016/j.fuel.2012.01.064>
- [18] Nickerson, T. A., Hathaway, B. J., Smith, T. M. and Davidson, J. H., Economic assessment of solar and conventional biomass gasification technologies: Financial and policy implications under feedstock and product gas price uncertainty, *Biomass and Bioenergy*, 2015, 74, 47-57. <https://doi.org/10.1016/j.biombioe.2015.01.002>
- [19] Lenis, Y. A., Pérez, J.F. and Melgar, A., Fixed bed gasification of Jacaranda Copaia wood: Effect of packing factor and oxygen enriched air, *Industrial Crops and Products*, 2016, 84, 166-175. <https://doi.org/10.1016/j.indcrop.2016.01.053>
- [20] Jangsawang, W., Laohalidanond, K. and Kerdsuan, S., Optimum equivalence ratio of biomass gasification process based on thermodynamic equilibrium model, *Energy Procedia*, 2015, 79, 520-527. <https://doi.org/10.1016/j.egypro.2015.11.528>
- [21] Porteiro, J., Patiño, D., Collazo, J., Granada, E., Moran, J. and Miguez, J. L., Experimental analysis of the ignition front propagation of several biomass fuels in a fixed-bed combustor, *Fuel*, 2010, 89 (1), 26-35. <https://doi.org/10.1016/j.fuel.2009.01.024>
- [22] Sharma, S. and Sheth, P. N., Air - steam biomass gasification: Experiments, modeling and simulation, *Energy Conversion and Management*, 2016, 110, 307-318. <https://doi.org/10.1016/j.enconman.2015.12.030>
- [23] Basu, P., "Biomass Characteristics," in *Biomass Gasification, Pyrolysis and Torrefaction*, Academic Press, Canada: Greenfield Research, Dalhousie University, 2018, pp. 49-91. <https://doi.org/10.1016/B978-0-12-812992-0.00003-0>
- [24] Ninduangdee P. and Kuprianov, V. I., Study on burning oil palm kernel shell in a conical fluidized-bed combustor using alumina as the bed material, *Journal of the Taiwan Institute of Chemical Engineers*, 2013, 44 (6), 1045-1053. <https://doi.org/10.1016/j.jtice.2013.06.011>
- [25] Montgomery, D. C., *Design and Analysis of Experiments*, 9th ed. Arizona: Wiley, 2017.
- [26] Bridgwater, A. V., The technical and economic feasibility of biomass gasification for power generation, *Fuel*, 1995, 74 (5), 631-653. [https://doi.org/10.1016/0016-2361\(95\)00001-L](https://doi.org/10.1016/0016-2361(95)00001-L)
- [27] Martínez, J. D., Mahkamov, K., Andrade, R. V. and Silva, E. E., Syngas production in downdraft biomass gasifiers and its application using internal combustion engines, *Renewable Energy*, 2012, 38 (1), 1-9. <https://doi.org/10.1016/j.renene.2011.07.035>

NOMENCLATURE

ER	Equivalence ratio (-)
HHV _{gas}	Syngas higher-heating-value (MJ/Nm ³)
HHV _{bms}	Biomass higher-heating-value (kJ/kg)
t _{Voff}	Shutdown time for hopper vibrating motor (s)
t _{Ron}	Operation time for ash removal motor (s)
t _{Roff}	Shutdown time for ash removal motor (s)
F _{air}	Airflow (Nm ³ /h)
\dot{m}_{gas}	Mass flow syngas (kg/h)
\dot{m}_{bms}	Biomass consumption rate (kg/h)
η_i	Efficiency (%)
E _{out}	Out energy the reactor in the syngas (kJ)
E _{in}	Input energy supplied in biomass (kJ)
ϵ_p	Biomass particle porosity (-)
ϵ_b	Biomass bulk porosity (-)
ρ_{real}	Real density (kg/m ³)
$\rho_{apparent}$	Apparent density (kg/m ³)
ρ_{bulk}	Bulk density (kg/m ³)
\bar{Y}	Response variables, average syngas higher-heating-value (MJ/Nm ³)
A	Mass percentage of Ash in the biomass, dry basis (%)
C, H, O, N and S	Mass percentages of Carbon, Hydrogen, Oxygen, Nitrogen and Sulfur respectively, in the biomass, dry basis (%)
H ₂ , O ₂ , N ₂ , CH ₄ , CO, CO ₂ and C ₂ H ₄	Gas concentration n/n (%)